RSC Advances

RSC Publishing

PAPER

View Article Online
View Journal | View Issue

Cite this: *RSC Adv.*, 2013, **3**, 23395

Facile synthesis of UV-white light emission ZnSe/ZnS:Mn core/(doped) shell nanocrystals in aqueous phase

Bich Thi Luong,[ab] Eunsu Hyeong,[a] Sujin Yoon,[a] Jongwan Choi[a] and Nakjoong Kim*[a]

Received 5th August 2013
Accepted 1st October 2013

DOI: 10.1039/c3ra44154g

www.rsc.org/advances

ZnSe/ZnS:Mn core/(doped) shell and ZnSe/ZnS:Mn/ZnS core/(doped) shell/shell nanocrystals (NCs) that emit white light were synthesized in aqueous media. White light emission of as-prepared NCs is a result of combined emission of blue light (emission from band gap of ZnSe core) and yellow/orange light ($^4T_1$–$^6A_1$ emission from Mn^{2+} ions doped in ZnS of the first shell). Especially, the green emission generated from surface defects was found as a key factor that affects the photoluminescence quantum yields of core/(doped) shell and core/(doped) shell/shell NCs. Photoluminescence from the Mn:ZnS d-dots was easily tuned from 580–600 nm by regulating feeding molar ratio [Zn]/[Mn]. Under the sufficiently low Mn^{2+} dopant concentration, ZnSe/ZnS:Mn and ZnSe/ZnS:Mn/ZnS NCs emit white light with a quantum yield about 27.6% and 20.5%, respectively.

Introduction

White-light emission from semiconductor nanostructures is presently a research area of interest due to their unique electrical, optical and chemical properties. Therefore, it is of great importance for many applications to find high-quality single source. White-light emitters through low-cost chemical synthesis approach which will allow the production of white light while meeting the needs of industry. Specifically, a need exists for efficient pure white light LED (light emitting diode) as a replacement for conventional lighting sources.[1] Presently, there are different methods to generate white light by three different paths according to three principles: (1) mixing fully visible light or mixing fully all visible phosphor nanocrystals (NCs); (2) combining green, red, and blue phosphor NCs; (3) combination of yellow and blue light. However, when the white light is generated by simply mixing phosphor NCs of different colors together, the observed efficiencies are often decreased due to the re-absorption of light and subsequent undesirable energy transfer. Thus, the undesirable changes in the chromaticity coordinate and photometric performance would be led due to the different relative temporal stabilities of the components. Hence the use at a single-emitting component offers many advantages over multiple component systems for white-light emitting sources such as LEDs, among which are greater reproducibility, lower cost preparation, ease of modification, simpler fabrication process. Recent research on quantum dots (QDs) that emit white light has been focused on cadmium chalcogenides by simply mixing red, green, and blue light from CdS, CdSe and CdTe QDs,[2,3] magic-sized CdSe QDs,[4] ultrasmall white-light emission CdSe (ref. 5) and manganese-doped sulfide QDs such as Mn:CdS, Mn:ZnS.[6–9] However, the intrinsic toxicity of cadmium, and the low total optical efficiency of cadmium chalcogenide QDs caused by self-absorption limit these QDs in large-scale applications.[10] The Mn-doped ZnSe d-dots core/shell that emit white light were synthesized by modifying a nucleation-doping strategy. Thus, the surface trap state emission of these QDs was realized and controlled.[11] The white light emission of manganese and copper co-doped ZnSe QDs were synthesized in a two-step process.[12] White emission was realized for Mn-doped ZnS NCs which synthesized in aqueous-phase.[13]

The tunable color from yellow to orange emission of ZnSe/ZnS:Mn/ZnS core/(doped) shell/shell NCs synthesized in organic solvent[14] and in aqueous media with three-step single flask.[17] Since the blue light of ZnSe at 395–400 nm and surface trap emission at 500 nm wavelength have been found, the white emission was obtained when the Mn^{2+} ions concentration was doped low enough.[10] The model of schematic representation to different emissions from ZnSe/ZnS:Mn core/(doped) shell NCs is ascribed in Fig. 1. Herein, we report the most green and simple synthetic route to produce ZnSe/ZnS:Mn core/(doped) shell and ZnSe/ZnS:Mn/ZnS core/(doped) shell/shell NCs that emit white light in aqueous medium. The mechanism is illustrated in Fig. 2, the blue circle elucidates the ZnSe core that emits blue light, the green layers represent the surface defects that give out green trap-state emission, the yellow layer

[a]*Organic Photonic and Electronic Materials Lab, Department of Chemistry and Research Institute for Natural Sciences, Hanyang University, 17 Haengdang-Dong, Seongdong-Gu, Seoul, 133-791, South Korea. E-mail: marialuongbich@gmail.com; kimnj@hanyang.ac.kr; Fax: +82-2-2295-0572; Tel: +82-2-2220-0935*

[b]*Institute of Applied Materials Science, Vietnam Academy of Science and Technology, 01 Mac Dinh Chi Street, Ben Nghe Ward, Ho Chi Minh City, Vietnam. Fax: +84-8-3823-6073; Tel: +84-8-3823-7927*

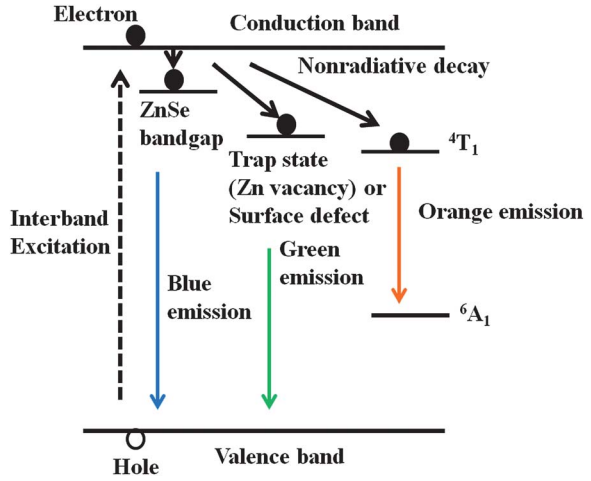

Fig. 1 Schematic representation of the model ascribed to different emission from ZnSe/ZnS:Mn and ZnSe/ZnS:Mn/ZnS NCs.

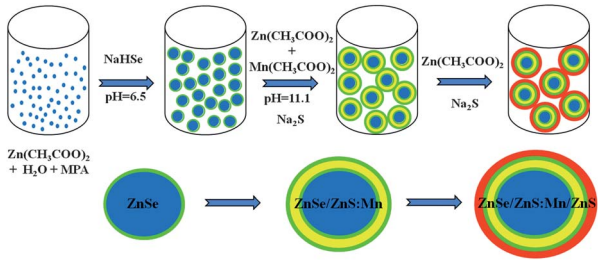

Fig. 2 Schematic illustration of reaction mechanism of white luminescent ZnSe/ZnS:Mn core/(doped) shell and ZnSe/ZnS:Mn/ZnS core/(doped) shell/shell NCs in aqueous media.

illustrates the ZnS:Mn doped shell that has the yellow/orange emission of Mn^{2+} ions, and the red layer explains the outer ZnS shell formation.[17] The reaction time, and dopant concentration were controlled to obtain white-light emission core/shell/shell NCs. The structure, growth mechanism and optical properties of core/multi-shell with Mn:ZnS d-dots at the first shell are studied in detail.

Experimental

Chemicals

All the chemicals are of analytical grade, purchased from Sigma-Aldrich, and were used without further purification. Manganese(II) acetate ($Mn(OAc)_2$) (Mn $(CH_3COO)_2 \cdot 4H_2O$, 99.99%), zinc acetate ($Zn(OAc)_2$) (Zn $(CH_3COO)_2 \cdot 2H_2O$, 99.99%) and sodium sulfide (Na_2S), 3-mercaptopropionic acid (MPA, 99+%), sodiumborohydride ($NaBH_4$, 96%), selenium powder (99.5%), 2-propanol (HPLC grade). Water (deionized water-DI water) used in all synthesis was high purity grade with a conductivity of 18.2 MΩ cm^{-1}.

Synthesis of ZnSe/ZnS:Mn core/(doped) shell and ZnSe/ZnS:Mn/ZnS core/(doped) shell/shell NCs

A literature synthetic method of NaHSe solution that mixed with Zn^{2+} ionic solution to form ZnSe core NCs at the first step was used as previous report.[15,16] The precursor of Zn^{2+} ionic solution for ZnSe core formation was prepared by dissolution 10 ml of zinc acetate 0.1 M in 90 ml of water, and 40 ml of MPA 0.1 M in three-neck flask, then the pH of this system was adjusted to pH = 6.5 using NaOH 2 M with vigorous stirring. This three-neck flask was degassed by N_2 bubble in 30 minutes, and then the NaHSe solution was injected into the Zn^{2+} precursor solution at room temperature under N_2. The system was heated to 90–100 °C and refluxed for 3 and 6 hours to optimize the refluxing time of the first ZnSe core growth step. At the second step of doping Mn^{2+} into ZnS shell and coating onto ZnSe core by following process. The previous three-flask reaction system was cooled to room temperature, then mixture of 7.9 ml of zinc acetate 0.1 M and 8.6 ml of manganese acetate 0.01 M (11.0% relative to Zn of the first shell) was dropwised at one drop per second into flask reaction. In order to get the desirable Mn-dopant concentrations (Mn^{2+} at% relative to Zn^{2+} of the first shell from 1.0 to 10.0% or upto 60.0%), concentrations and volumes of manganese acetate were adjusted, and the temperature was raised to 80.0 °C, then the pH of reaction system was adjusted to 11.1 by NaOH 2 M to form majority S^{2-} anions in solution after 8.7 ml of Na_2S 0.1 M was injected slowly for ZnSe/ZnS:Mn core/(doped) shell NCs formation. The reaction flask was stirred for one and half hours to get the faint white emission visible under UV light with 365 nm wavelength, then it was cooled to room temperature and prepared for further measurement or kept on stirring for the third ZnS growth step. In order to compare the photoluminescence quantum yields (PL QYs) of ZnSe/ZnS:Mn core/(doped) shell NCs and ZnSe/ZnS:Mn/ZnS core/(doped) shell/shell NCs, the ZnS layer was coated onto the ZnSe/ZnS:Mn core/(doped) shell NCs at the third step. Thus, the reaction system of ZnSe/ZnS:Mn core/(doped) NCs was kept on stirring at 90 °C, then 8.3 ml of zinc acetate 0.1 M was added slowly and 8.3 ml of Na_2S 0.1 M was doped to obtain ZnS outer shell layer coated onto ZnSe/ZnS:Mn core/(doped) shell NCs to form ZnSe/ZnS:Mn/ZnS core/(doped) shell/shell NCs. The system was continuously stirred for further different hours to compare the PL QYs and intensities of different as-prepared NCs samples. This synthetic method was briefly mentioned in previous research.[17]

Characterization

The obtained suspension was concentrated to one-tenth of the original volume, and then the NCs were precipitated in 2-propanol, washed and collected *via* centrifugation and decantation, finally dried in a vacuum. The obtained powder was used for characterization. UV-vis absorption spectra were using an Optizen 2120UV spectrophotometer (Science and Technology development). Fluorescence measurements were carried out at room temperature. The PL QY of NCs was measured according to the method described in Crosby and Demas.[18] PL QYs were determined by comparing the integrated emission of the NCs samples in water with that of fluorescent dye rhodamine 6G (PL QY = 95% in ethanol) with identical optical density (0.05–0.01) at the excitation wavelength. A D/Maxrint 2000 powder diffractometer with Cu Kα radiation

(λ = 1.5418 Å) was used to perform X-ray diffraction measurements. The X-ray photo electron spectra (XPS) were taken on a Thermo scientific K-alpha electron energy spectrometer using Al Kα (1486.6 eV) as the X-ray excitation source (VG Multi-lab ESCA 200 system model). High resolution transmission electron (HRTEM) micrograph image was acquired using a TEM 2100F with acceleration voltage of 200 kV. TEM samples were prepared by dropping the samples dispersed in water onto carbon coated copper grids with excess solvent evaporated. The average size of NCs was determined using J-image software from TEM images.

Result and discussion

Influence of experimental parameters

The optimal reaction conditions to produce ZnSe/ZnS:Mn core/(doped) shell and ZnSe/ZnS:Mn/ZnS core/(doped) shell/shell NCs with white light emission were determined.

White light emission mechanism of ZnSe/ZnS:Mn core/shell NCs and ZnSe/ZnS:Mn/ZnS core/shell/shell NCs

The white light emission is theoretically the combination of yellow and blue light. Nevertheless, in this work the green luminescent emission of surface defects appear to favor the generation of white light after incorporation of the Mn ions into the host ZnS lattice in the second step of ZnS:Mn shell deposition onto the ZnSe core. And this result was found to be related to previous research.[12] Hence, the white light emission of ZnSe/ZnS:Mn core/shell and ZnSe/ZnS:Mn/ZnS core/shell/shell NCs is the result of a well-controlled combination of emission of yellow/orange light given by Mn^{2+} based $^4T_1$ to $^6A_1$ transition of doped shell ZnS:Mn coated onto the ZnSe core, the green light from surface defects and blue light from band gap of ZnSe core (Fig. 1). The ZnS thin outer layer is the layer to increase the photo stabilizer due to preventing the energy transfer to surface states or surrounding medium and migration of the Mn dopant.[7,17,19] Actually, the ZnSe core NCs have two emission peaks that are the emission of deep trap of ZnSe due to the suitable band gap (400–420 nm),[15,20] and another peak at 500–520 nm wavelength of surface trap emission of ZnSe stabilized by MPA capping agent synthesized in aqueous phase (see Fig. 3).[17] For two ZnSe as-prepared samples at three and six hours of refluxing have similar PL intensities, the refluxing time at three hours was chosen to go on with other experiments. Since the Mn^{2+} contain is high enough, the yellow or orange/red emission could be obtained.[17] That the PL spectrum of ZnSe NCs after 6 hours refluxing shows a new peak around 365 nm compared to that refluxed for 3 hours is assigned to the excitonic emission.[36] The excitonic emission occurs with a new peak after 6 hours reflux due to the lightly increasing size of sample 6 hours reflux which causes the reducing of dielectric constant of sample, so the exciton is more increased.[38] The 3 hours reflux sample has no peak of excitonic emission due to the domination of blue and green emissions.[37,38]

More interestingly, the low enough Mn^{2+} dopant concentrations were added, the white emission of the ZnSe/ZnS:Mn/ZnS core/shell/shell NCs was obtained due to the well-controlled intensity of blue, green and yellow/orange/red emissions so that the UV-white light was shown at the three emissions at different wavelength in PL spectra (Fig. 4). Thus, the feeding molar ratio [Zn]/[Mn] is the most important parameter that affects on the color-tunable emission.[11]

When the Mn^{2+} dopant is sufficient to the core/multi-shell emits white light, the PL spectra of the as-prepared ZnSe/ZnS:Mn/ZnS NCs that emit white light shown in Fig. 4(a) and 6. The quantum yields (QYs) of these as-prepared NCs were about 20.5% (11.0% Mn-doped) and 18.6% (10.0%) which were calculated according to the reported method.[13]

ZnSe/ZnS:Mn core/shell NCs and ZnSe/ZnS:Mn/ZnS core/shell/shell NCs probably have three emissions. These luminescent features of the emission spectra attributed to emission from energetically different midgap states. The peak at 400–420 nm is assigned to the band gap of ZnSe.[15,20] The peak at 500–520 nm is assigned to trap state emission from surface defects.[21–25] The feature at 583–600 nm is assigned to the pseudo-tetrahedral ($^4T_1$ to $^6A_1$) transition of Mn^{2+} ions incorporated into the ZnS d-dot emission results from the recombination of an electron and hole, while trap emission is the result of recombination between a photogenerated hole trapped in a midgap state and an electron.[4] The green synthesis ZnSe/ZnS:Mn core/shell and ZnSe/ZnS:Mn/ZnS core/shell/shell NCs using MPA as a stabilizer in aqueous media by suitable feeding molar ratio between Zn and Mn, rapid mixing speed, temperature and other precise control over parameters[26] means that it allows the surface structure of d-dots to be easily modified to obtain trap state emission. The appropriate combination of yellow light (Mn^{2+}-based $^4T_1$ to $^6A_1$ emission) and blue light (trap state emission) produces white light.

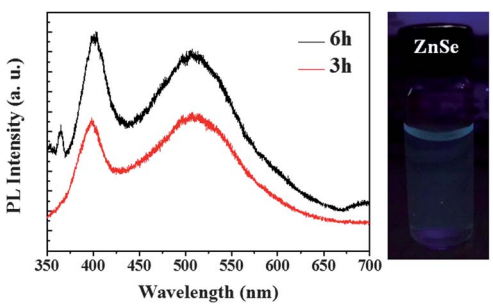

Fig. 3 PL spectra of ZnSe NCs in water and photograph of ZnSe (3 refluxing hours) under UV light (365 nm).

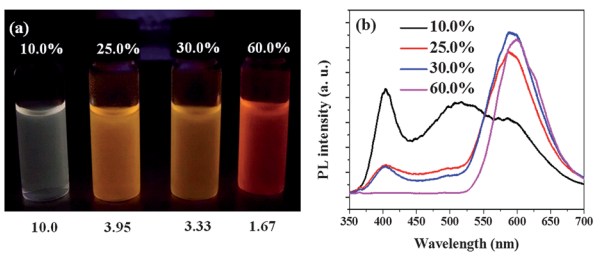

Fig. 4 (a) Photographs under a UV lamp (365 nm) and (b) PL spectra of four color-tunable ZnSe/ZnS:Mn/ZnS core/(doped) shell/shell NCs samples from white to red.

Influence of the [Mn] was set larger than 14.3, the/[Mn]

The concentration of zinc acetate 0.1 M and manganese acetate 0.01 M are kept constant (while doping low Mn concentration from 1.0 to 15.0%), the percent of Mn^{2+} dopant relative to Zn^{2+} of the first doped shell was adjusted by changing the volume of manganese acetate and keeping constant zinc acetate volume. As previous researches[14] reported that the flowing rate of precursor solution was poured at 1 drop per second for well-doped Mn^{2+} into the ZnS crystalline after adding S^{2-} anions precursor. At low Mn-dopant concentration, the surface defects are significantly affected by the different size of Mn^{2+} and Zn^{2+} ions while the yellow/orange emission of Mn-dopant is mainly remained at high Mn-dopant concentration due to the strongest transition of d-dots Mn^{2+} impurity (Fig. 4–6).[17,20] With the further thickening of the ZnS outer shell by longer refluxing time, the lattice mismatch between the ZnS:Mn doped shell and the ZnS outer shell materials results in the formation of defects that leads to the nonradiative recombination.[20]

Different ratios of feeding moles [Zn]/[Mn] causes the various PL intensity and position of emission peaks. When the feeding molar ratio of [Zn]/[Mn] was set larger than 14.3, the peaks at 400–420 nm and 500–520 nm are shown in Fig. 5 and the blue peak is little more intense than that of green emission and the fluorescence emission under ultraviolet lamp was blue (see Fig. 6). When the molar ratio of [Zn]/[Mn] was set 10.0–14.3, the PL intensity of the peak at 580 nm is appeared and the peak at 500–520 nm is increased significantly. As a result, the overall difference in PL intensity between the peaks was very small, and white light emission was observed. In contrast, when the feeding molar ratio of [Zn]/[Mn] was set from 8.7 or less than 8.7, the emission at 580 nm is dramatically increased, and there is almost emission from the Mn^{2+}-based $^4T_1$ to $^6A_1$ transition was observed when the molar ratio [Zn]/[Mn] reduces to 5.0 (see Fig. 5), the trap-state and surface state emission almost vanished, and the light emitted was yellow due to the higher Mn^{2+} dopant concentration.[17] The peak intensity at 580 nm seems to be affected by the ratio of [Zn]/[Mn]. It changes monotonically with doping Mn from 3.0% ([Zn]/[Mn] = 33.3) to 45.0% ([Zn]/[Mn] = 2.22) except sample 11.5% ([Zn]/[Mn] = 8.70). This situation could be explained by the transitional phase between white light and yellow emissions. The intermediate point of increasing and decreasing of molar ratio [Zn]/[Mn], so the surface trap state emission (500–520 nm) is reduced while yellow emission (580 nm) is suddenly increased due to the number of non-coordinated surface selenium and sulfur sites decreased.[11] The linear increasing of 580 nm emission peaks with Mn doping concentration is caused by the increasing of number Mn dopant for higher luminescent enhancement.

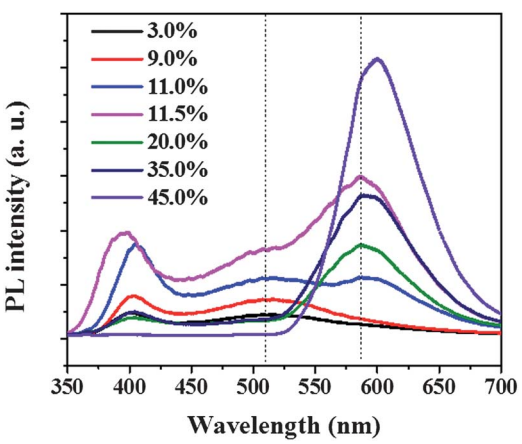

Fig. 5 The PL spectra of tunable samples from blue to orange of core/(doped) shell/shell NCs.

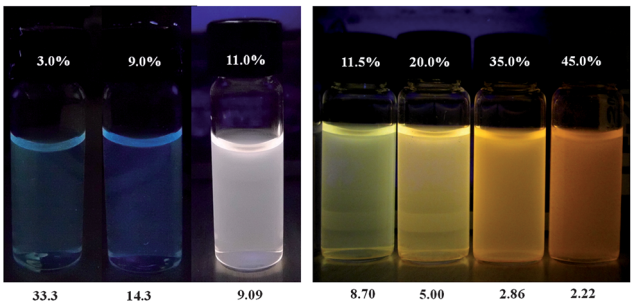

Fig. 6 Photographs of tunable core/(doped) shell/shell NCs samples from blue to orange under a UV lamp (365 nm).

Synthesis mechanism of ZnSe/ZnS:Mn core/shell NCs and ZnSe/ZnS:Mn/ZnS core/shell/shell that emit white light

In our work, white light emission from Mn^{2+}-doped ZnS d-dots was the result of a combination of emission of yellow/orange light (Mn^{2+}-based $^4T_1$ to $^6A_1$ emission), green emission of surface defects, and blue light. If the purpose is to obtain high quality d-dots with white light emission, the optical properties of these three emission features need to be controlled. Generally speaking, the optical properties of Mn^{2+}-doped ZnS shell d-dots a mutually diffuse Zn/Mn interface (to achieve Mn^{2+}-based $^4T_1$ to $^6A_1$ emission), and surface trap states. The size and interface with mutually diffuse Zn/Mn ions both have a large impact on yellow emission, a detailed explanation of which has been presented previously.[27] In general, the presence of surface defects is the result in trap state emission should be avoided in the synthesis of fluorescent d-dots. However, for these Mn^{2+}-doped ZnS d-dots of the ZnSe/ZnS:Mn/ZnS core/shell/shell NCs that emit white light, the blue emission from band gap of ZnSe core and surface trap state (green emission) were required to achieve white light emission. The white emission is assigned when three emissions at 400–420, 500–520 nm due to the surface trap states, and 580–600 nm are appeared and well-controlled intensities. To formulate a mechanism for the formation of surface trap states, a fundamental understanding of the structure of the d-dots is required.

The optical properties of d-dots are the result of quantum confinement and that the competitions between radiative and non-radiative pathways mainly depends on the separation between an impurity and the surface or other impurities.[27–30] In our work, the small size of the NCs means that quantum size and surface effects dominate the optical properties of the d-dots

because most atoms are on their surface, which results in reduced coordination between atoms, and more dangling bonds. The presence of point defects (vacancies or interstitial atoms) from the different ionic sizes of Zn^{2+} and Mn^{2+} could introduce surface trap states that allow the recombination of an electron and hole, resulting in white emission due to increasing the trap state emission at 500–520 nm. This proposition is supported by the presence of surface trap states in selenium hydrate NCs as reported by Underwood *et al.*[24,25] ZnSe core NCs have two features that blue emission (390–420 nm) is from ZnSe band gap and green emission (500–520 nm) is a result of recombination of electrons and holes at surface trap states or which is induced by hole-trapping thiolates on the NC surface or the zinc-vacancy from different ionic size of Zn^{2+} and Mn^{2+} cations.[31] The green multi-step synthesis in aqueous phase in single flask with using MPA as a stabilizer allows the adjustment of feeding molar ratio of [Zn]/[Mn], so the white light emission was obtained and controlled. The MPA concentration and the mechanism synthesis to produce ZnSe/ZnS:Mn/ZnS core/shell/shell NCs in aqueous phase was mentioned as previous report.[17] At low Mn^{2+} dopant concentration, it may not affect the sizes of the core/shell/shell NCs by prolong growth time of doping at the first doped shell ZnS:Mn of ZnSe/ZnS:Mn and ZnSe/ZnS:Mn/ZnS NCs. Therefore, the surface trap state is more significant due to Zn^{2+}, Mn^{2+} ionic sizes difference. When the feeding molar ratio [Zn]/[Mn] is large enough [>14] not to have white emission, so an excess of Zn^{2+} ions causes non-coordinated surface sulfide (selenium) sites to form and the blue emission is mainly obtained. Conversely, the ratio [Zn]/[Mn] is at a range of [9.0–10.0] to obtain white light emission due to either three luminescent intensities of Mn^{2+}-based yellow emission and green trap state emission and blue band gap emission became almost well-balanced of ZnSe/ZnS:Mn (11.0%)/ZnS core/(doped) shell/shell NCs or blue and green emission intensities are mostly equal of ZnSe/ZnS:Mn (11.0%) core/(doped) shell NCs (Fig. 7), combining to produce white light. When the molar feeding ratio of [Zn]/[Mn] is decreased (less than 9.0), the surface structure of samples improved, and the number of non-coordinated surface selenium (sulfide) sites decreased, and so the intensity of surface trap state emission decreased, while that of Mn^{2+}-based $^4T_1$ to $^6A_1$ emission increased, causing the PL to red shift due to the magnetic interaction Mn–Mn ions in one crystal since the more amount of Mn^{2+} ions.[10] When the molar ratio [Zn]/[Mn] was further decreased, the concentration of Zn^{2+} ions was insufficient to meet the demands of shell growth, causing a mutually diffuse [Zn]/[Mn] interface to form on the surface of samples. Such a surface possesses Mn^{2+} dangling bonds, which cause fluorescence self-quenching and decreasing PL QY.[17]

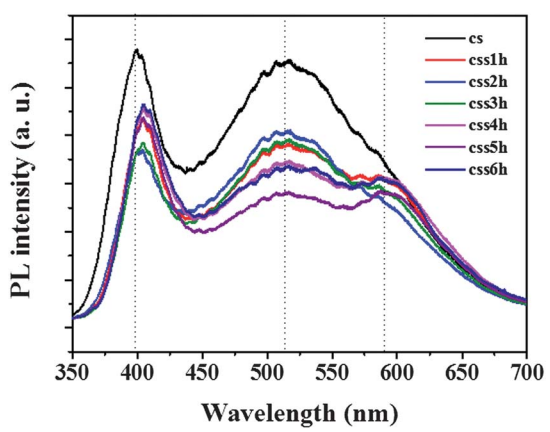

Fig. 7 The PL spectra of ZnSe/ZnS:Mn (11.0%) core/(doped) shell and ZnSe/ZnS:Mn (11.0%)/ZnS core/(doped) shell/shell NCs in water.

In this case of white light emission using low doping Mn^{2+} concentration, the formation of ZnS shell makes the PL QY reduced due to the decrease of surface trap emission from zinc-vacancy and surface states of ZnS:Mn doped shell of ZnSe/ZnS:Mn core/(doped) shell NCs. The PL QY of ZnSe/ZnS:Mn (11.0%) core/(doped) shell NCs and ZnSe/ZnS:Mn (11.0%)/ZnS core/shell/shell NCs are 27.6% and 20.5%, respectively (see Fig. 7). Herein, the emit white light with a higher quantum yield about 27.6% is higher than previous report.[11] The ZnSe/ZnS:Mn (11.0%) core/shell NCs have two emissions with green emitting intensity that is almost equal to blue emission, so the light emitting intensity is the strongest. There are a number of different transition mechanisms involved in the emission of the ZnSe/ZnS:Mn core/(doped) shell system. After electrons have been excited from the valence band to valence band of ZnS host in Mn-doped into ZnS host system and ZnSe core system has the same principle, a number of electrons may relax to the defects states, from where they can recombine with holes in the valence band, with the resultant emission of photons in the 500–520 nm spectral region. When the manganese ions are present, some of them are adsorbed on the surface of the doped NCs and hence populate these surface sites. Therefore, radiative recombination between electrons in the defect states and holes in the d orbitals of the manganese ions is expected to increase in dominance. Hence significantly, the peak intensity of the defect state-related (green emission) PL overlapped Mn^{2+}-related d–d emissions of ZnSe/ZnS:Mn (11.0%) core/(doped) shell as-prepared NCs and increased more intensely compared with Mn^{2+}-related d–d emissions of ZnSe/ZnS:Mn (11.0%)/ZnS core/(doped) shell/shell NCs (Fig. 7).

The MPA added has two important roles in trap state emission due to ZnS thin layer formation. As this ZnS layer formation, three emission features appear in PL spectra due to the competition of Mn^{2+} transition ($^4T_1$ to $^6A_1$) and surface trap state transition (green emission), the green emission is lightly reduced (Fig. 7). Fig. 8 shows photographs of ZnSe core with blue emission, ZnSe/ZnS:Mn (11.0%) core/shell and ZnSe/ZnS:Mn (11.0%)/ZnS core/shell/shell NCs in water under UV light (wavelength = 365 nm). MPA-like ligands have unique "secondary coordination" and longer chains to allow the most energetically favorable hexagonal configuration with ions on the surface to form, which promoted Mn^{2+}-based $^4T_1$ to $^6A_1$ yellow emission. Furthermore, one molecule of MPA can coordinate to one metal ion atom site to form the most favourable hexagonal configuration, enhancing the colloidal stability of the formed NCs and this favourable for PL performance. Thus, the MPA is great enough for light emission and good

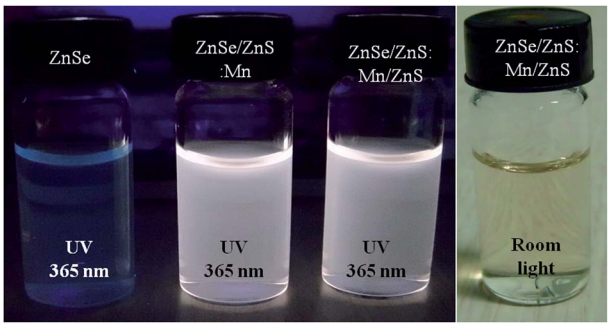

Fig. 8 Photographs of ZnSe core, ZnSe/ZnS:Mn (11.0%) core/(doped) shell and ZnSe/ZnS:Mn (11.0%)/ZnS core/(doped) shell/shell NCs in water under a UV lamp (365 nm).

water-dispersion of either core/(doped) shell or core/(doped) shell/shell NCs. Overall, both the feeding molar ratio of [Zn]/[Mn] and mass of adding MPA influence the optical properties of ZnSe/ZnS:Mn and ZnSe/ZnS:Mn/ZnS NCs that emit white light.

Structural characterization of ZnSe/ZnS:Mn/ZnS NCs

Fig. 9(a) shows the wide-angle XRD patterns of the as-prepared ZnSe core, ZnSe/ZnS:Mn (11.0%) core/shell and ZnSe/ZnS:Mn (11.0%)/ZnS core/shell/shell. The three main peaks that correspond to the (111), (220) and (311) planes, respectively, showing that the as-prepared core, core/shell and core/shell/shell NCs have a cubic (zinc blend) structure mainly. Meanwhile, it supports the hypothesis that Mn^{2+} is more facile to incorporate in cubic ZnS NCs more than wurtzite and rock-salt crystals.[17,33] Moreover, the doping Mn^{2+} into the host ZnS of the first shell NCs of core/multi-shell NCs does not totally bring about a phase transformation of the crystal structure. However, there are several sharp peaks appeared in the XRD pattern of CS (11%) and CS (11%) S samples. This could be explained that two phases of zinc-blend and hetaerolite were formed, but the hetaerolite is minor and the phase transformation is appeared secondary.[37] We found that the diffraction peaks shifted to a larger angles as the shell increasing thickness.[34,35] Fig. 9(b) is the TEM images of ZnSe/ZnS:Mn (11.0%) shows that the distribution is good. The average size of core/(doped) shell NCs (5.3 ± 0.2 nm) is larger than ZnSe core (4.6 ± 0.2 nm).[17] The XPS spectra of ZnSe core, ZnSe/ZnS:Mn (11.0%) core/shell, and ZnSe/ZnS:Mn (11.0%)/ZnS core/shell/shell NCs are shown in Fig. 9(c) and (d). The binding energy assigned to S 2p shifted from 163.0 eV for the ZnSe NCs to 162.0 eV for the ZnSe/ZnS:Mn (11.0%) and ZnSe/ZnS:Mn (11.0%)/ZnS NCs, which verified the proposed core/shell/shell structure and was consistent with previous reports.[17,32] Furthermore, Fig. 9(d) provides further evidence for growth of the ZnS:Mn(S) on the ZnSe core, and ZnS shell on the ZnSe/ZnS:Mn (11.0%) core/shell NCs. The XPS information of Zn intensity has been lightly increase from ZnSe core, to ZnSe/ZnS:Mn (11.0%) core/shell and ZnSe/ZnS:Mn/ZnS core/shell/shell NCs due to the layers of the shell increase. It is shown in Fig. 9(d) that the Zn concentration is increased in the core NCs, core/shell NCs and core/shell/shell NCs.

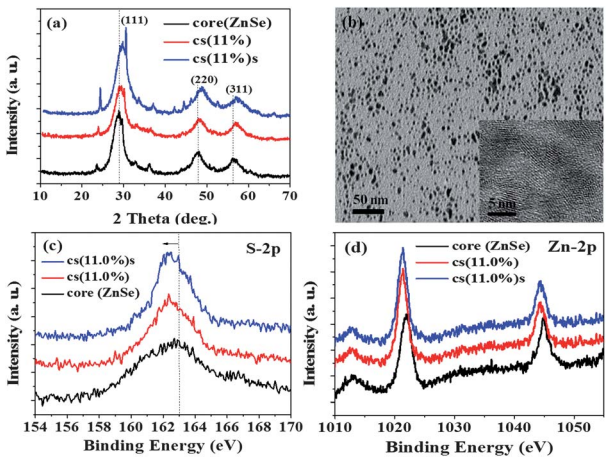

Fig. 9 (a) XRD patterns, and (c and d) XPS spectra of ZnSe core, ZnSe/ZnS:Mn (11.0%) core/shell – cs (11.0%), ZnSe/ZnS:Mn (11.0%)/ZnS core/shell/shell – cs (11.0%)s NCs (b) TEM images of ZnSe/ZnS:Mn (11.0%) – cs (11.0%) NCs.

Conclusions

In summary, we report white light emission of water-soluble ZnSe/ZnS:Mn core/(doped) shell and ZnSe/ZnS:Mn/ZnS core/(doped) shell/shell NCs synthesized by a green and facile method in aqueous phase. The obtained NCs give out the white emission with using Mn^{2+} d-dots at a range of feeding concentration 10.0–11.0% relative to Zn of the d-dot shell (doped shell) related to a range of feeding molar ratio [Zn]/[Mn] from 9.0 to 10.0 and possess a high degree of crystallinity, good quantum efficiencies, and narrow size distribution, making them potential candidates for white LEDs, and biological labels.

Acknowledgements

This work was supported by the National Research Foundation of Korea (NRF) grant funded by the Korea government (MSIP) through the Active Polymer Center for Pattern Integration (no. 2007-0056091).

Notes and references

1 J. Y. Tsao, *Light Emitting Diodes (LEDs) for General Illumination-an OIDA Technology Roadmap Update*, 2002, http://www.netl.doe.gov/ssl/publications.html.
2 J. Lee, V. C. Sundar and J. R. Heine, *Adv. Mater.*, 2000, **12**, 1102–1105.
3 A. Lita, A. L. Washington II, L. Burgt, G. F. Strouse and A. E. Stiegman, *Adv. Mater.*, 2010, **22**, 3987–3991.
4 M. J. Bowers II, J. R. McBride and S. J. Rosenthal, *J. Am. Chem. Soc.*, 2005, **127**, 15378–15379.
5 T. E. Ronsson, S. M. Claiborne, J. R. McBride, B. S. Stratton and S. J. Rosenthal, *J. Am. Chem. Soc.*, 2012, **134**, 8006–8009.
6 A. Nag and D. D. Sarma, *J. Phys. Chem. C*, 2007, **111**, 13641–13644.

7 S. Kar and S. Biswas, *J. Phys. Chem. C*, 2008, **112**, 11144–11149.
8 X. D. Lü, J. Yang, Y. Q. Fu, Q. Q. Liu and B. Qi, *Nanotechnology*, 2010, **21**, 115702–115711.
9 H. Z. Wang, H. Nakamura, M. Uehara, Y. Yamaguchi and M. Miyazaki, *Adv. Funct. Mater.*, 2005, **15**, 603–608.
10 A. H. Mueller, M. A. Petruska, M. Achermann, D. J. Werder, E. A. Akhadov, D. D. Koleske, M. A. Hoffbauer and V. I. Klimov, *Nano Lett.*, 2005, **5**, 1039–1044.
11 P. Shao, H. Z. Wang, Q. H. Zhang and Y. G. Li, *J. Mater. Chem.*, 2011, **22**, 17972–17977.
12 S. K. Panda, S. G. Hicky, H. V. Demir and A. Eychmüller, *Angew. Chem., Int. Ed.*, 2011, **50**, 4432–4436.
13 N. Pradhan and X. G. Peng, *J. Am. Chem. Soc.*, 2007, **129**, 3339–3347.
14 R. Thakar, Y. C. Chen and P. T. Snee, *Nano Lett.*, 2007, **7**, 3429–3432.
15 A. Shavel, N. Gaponik and A. Eychmüller, *J. Phys. Chem. B*, 2004, **108**, 5905–5908.
16 D. L. Klayman and T. S. Griffin, *J. Am. Chem. Soc.*, 1973, **95**(1), 197–199.
17 B. T. Luong, E. S. Hyeong, S. H. Ji and N. J. Kim, *RSC Adv.*, 2012, **2**, 12132–12135.
18 J. N. Demas and G. A. Crosby, *J. Phys. Chem.*, 1971, **75**, 991–1024.
19 Y. Yang, O. Chen, A. Angerhofer and Y. C. Cao, *J. Am. Chem. Soc.*, 2006, **128**, 12428–12429.
20 Z. Fang, P. Wu, X. Zhong and Y. J. Yang, *Nanotechnology*, 2010, **21**, 305604–305609.
21 C. Wang, X. Gao, Q. Ma and X. G. Su, *J. Mater. Chem.*, 2009, **19**, 7016–7022.
22 Y. L. Guo, W. L. Yang, F. H. Yu and T. C. Huan, *J. Mater. Chem.*, 2007, **17**, 2661–2666.
23 T. J. Norman Jr, D. Magana, T. Wilson, C. Burns and J. Z. Zhang, *J. Phys. Chem. B*, 2003, **107**, 6309–6317.
24 N. A. Hill and K. B. Whaley, *J. Chem. Phys.*, 1994, **100**, 2831–2837.
25 D. F. Underwood, T. C. Kippeny and S. J. Rosenthal, *J. Phys. Chem. B*, 2001, **105**, 436–443.
26 X. X. Zhu, Q. H. Zhang, Y. G. Li and H. Z. Wang, *J. Mater. Chem.*, 2008, **18**, 5060–5062.
27 P. T. Shao, Q. H. Zhang, Y. G. Li and H. Z. Wang, *J. Mater. Chem.*, 2011, **21**, 151–156.
28 N. Pradhan, D. Goorskeym, J. Thessing and X. G. Peng, *J. Am. Chem. Soc.*, 2005, **127**, 17586–17587.
29 H. Zhang, L. P. Wang, H. M. Xiong, L. H. Hu, B. Yang and W. Li, *Adv. Mater.*, 2003, **15**, 1712–1715.
30 Z. Y. Tang, N. A. Kotov and M. Giersig, *Science*, 2002, **297**, 237–240.
31 Z. Deng, F. L. Lie, S. Shen, I. Ghosh, M. Mansuripur and A. J. Muscat, *Langmuir*, 2009, **25**, 434–442.
32 Y. He, H. T. Lu, L. M. Sai, Y. Y. Su, M. Hu, C. H. Fan, W. Huang and L. H. Wang, *Adv. Mater.*, 2008, **20**, 3416–3421.
33 S. C. Erwin, L. Zu, M. I. Haftel, A. L. Efros, T. A. Kennedy and D. J. Norris, *Nature*, 2005, **436**, 91–94.
34 B. Dong, L. Cao, G. Su and W. Liu, *Chem. Commun.*, 2010, **46**, 7331–7333.
35 D. Zhu, X. X. Jiang, C. Zhao, X. L. Sun, J. R. Zhang and J. J. Zhu, *Chem. Commun.*, 2010, **46**, 5226–5228.
36 N. Murase and M. Gao, *Mater. Lett.*, 2004, **58**, 3898–3902.
37 E. Sotelo-Gonzalez, L. Roces, S. Garcia-Granda, M. T. Fernander-Arguelles, J. M. Costa-Fernandez and A. Sanz-Medel, *Nanoscale*, 2013, **5**, 9156–9161.
38 I. Pelant and J. Valenta, *Luminescence Spectroscopy of Semiconductors*, Oxford University Press, Oxford, 2012, ch. 7, pp. 161–204.